5-2014

# Optimizing in vitro extracellular matrix production using polymer scaffolds with targeted pore size

Addison M. Walker
*University of Arkansas, Fayetteville*

This thesis is approved.

**Thesis Advisor:**

**Thesis Committee:**

# *Optimizing in vitro Extracellular Matrix Production Using Polymer Scaffolds with Targeted Pore Size*

An Undergraduate Honors College Thesis

In the

Department of Biomedical Engineering
College of Engineering
University of Arkansas
Fayetteville, AR

By

Addison Martin Walker

## Introduction

Tissue regeneration is a rapidly expanding field concentrated on promoting the proper healing and return of function to tissue after experiencing injury or disease. Within this field, the development of novel biomaterials for scaffolds optimizes cell growth and organization optimizing recovery of the injured tissue [1]. Extracellular matrix (ECM) acts as the backbone for cell structure and organization. ECM plays a critical role in all tissues in providing structure for cell growth after cells experience injury [2]. To understand its role, one must first look at the composition of ECM. ECM is primarily composed of collagen providing the anchoring of cell structure. Fibronectin is another important component in the ECM that promotes cell attachment [3]. Laminin is another adhesion protein found in the ECM that further promotes angiogenesis within the healing tissue. Finally, glycosaminoglycans (GAG) function to bind to both cell surface receptors and growth factors [3]. When tissue experiences injury, it is of high importance for the tissue to have scaffolding like ECM in place for proper healing.

In designing a scaffold, the goal is to create a three dimensional porous network for cells to attach. Scaffolds must be biocompatible, have appropriate mechanical strength, and contain biological signaling factors to promote tissue regeneration [4]. Overall, degradable synthetic polymers are the most commonly used scaffolding material in tissue regeneration. However, synthetic polymers have distinct disadvantageous. The body elicits an inflammatory response to foreign bodies recognizing synthetic polymers as such. If polymers are not degraded, the effected tissue will be in a state of chronic inflammation constantly destroying and remodeling tissue in an effort to rid the body of the scaffold. This can lead to build up of scar tissue and tissue death [5]. Many critical biological signals are also not found in synthetic polymers, making the scaffold less effective [4]. In place of synthetic polymer scaffolds, natural scaffolds using ECM have been reported [6], [7]. Natural ECM scaffolds have the distinct advantage of being composed of the same molecules found in the body. Some variance occurs from tissue to tissue, but the composition remains similar across all tissues. Molecules that make up ECM are even conserved across different species making immune response to ECM scaffolds less likely [7]. The structure of cell derived ECM varies from tissue to tissue, but can be controlled for patients by culturing specific cell types [7]. The chosen cell type ideally will be the same as the targeted tissue for

regeneration. ECM scaffolds also contain important growth factors like VEGF to promote angiogenesis. The presence of natural growth factors further reduces the risk a foreign body response will occur [8]. The significance of this research is shown through the many applications of ECM scaffolds. ECM scaffolds can be used for skin grafts, esophagus reconstruction, bladder reconstruction, corneal repair, spinal cord repair, and ligament reconstruction [8].

In this project, the goal was to harvest ECM from decellularized cell cultures after culturing for three weeks. Removing cells from the original tissue or scaffold leaves behind the valuable ECM. As described, ECM plays a pivotal role in tissue regeneration. Previously, various methods have been used to produce and harvest ECM from cells. ECM has been harvested using open cell polyurethane (PU) scaffolds [6, 9]. However, this method has not studied the effects of the pore size of the PU scaffold on both ECM structure and ECM yield. We hypothesized that pore size would change the overall yield of ECM, but to what extent was not known.

The objective of this study is to first create PU scaffolds with targeted pore size by sieving sugar granules to specific ranges of granule size. The resulting scaffolds will then be characterized to show that the proposed procedure does in fact change the relative porosity and pore size of individual pores within each scaffold. If proven there is a significant difference in scaffold structure, cells will be cultured on the scaffolds. After three weeks the PU scaffold will be dissolved, and the resulting ECM yield will be measured. The results of this study will determine if the pore size of open cell polymer scaffolds effects the overall yield of ECM after decellularization.

## Materials and Methods

*Preparation of polymer molds of specific pore size*

Polymer scaffolds provided the structure needed to support cell growth. Previous methods in synthesizing scaffolds have been discussed and in general were followed; however, the prior methods did not seek to target specific pore size within the scaffold [6, 9]. To create the targeted pore size, culinary granulated

sugar was first placed in a U.S.A Standard Testing Sieve No. 35 (500um), then a No. 60 Sieve (250um), and finally a No. 120 Sieve (125um). This separated sugar granules of desired sizes of 125-250um and 250-500um. Beginning with the 125-250um sugar granule size, 10 grams of sugar was measured and mixed with 200uL of distilled water. The mixture was stirred until the sugar had the consistency of wet sand. The sugar was then loaded and packed into six cylindrical molds created using a small steel plate and a rubber slab attached with cylinders extruded. The molds were then placed in an oven set at 60°C for 20 minutes. This process was repeated with 250-500um granule sugar and unsieved sugar, which acted as the control group.

SC80a PU pellets were dissolved over night in dimethylacetamide (DMAC) (10%w/v) at 60°C and continuously stirred until time of use. Using a micropipette, the PU/DMAC solution was poured over each sugar mold drop by drop until saturated. Each mold required approximately 1mL. Any excess solution pooled in the mold was removed using a Kimwipe. The molds were then submersed in deionzied (DI) water for 24 hours. The water bath served to dissolve the sugar granules leaving behind voids where the sugar granules previously were. The created scaffolds were subject to three separate 24 hour DI water baths to remove sugar and DMAC, which is toxic to cell. The scaffolds were frozen to -80°C. In total, 6 scaffolds from sugar granules sized 125um-250um, 6 scaffolds from sugar granules sized 250-500um were created, and 12 control scaffolds from unsieved sugar granules were created.

*Characterization*

Polymer scaffolds were characterized both directly and using optical methods. First, physical measurements of each scaffold's diameter (mm) and height (mm) were taken using a digital caliper (data not shown). Each scaffold was then weighed (mg) using the AG204 Mettler Toledo Scale. The scaffolds were idealized to be perfect cylinders allowing a volume measurement. Porosity for each scaffold was measured using equation 1 [10]:

$$\Pi = 1 - \frac{\rho_{scaffold}}{\rho_{material}} \quad (1)$$

SG80a Polyurethane has a known density of 1.04 mg/mm$^3$ [11].

Scaffolds were then characterized using imaging software. The goal for using these images was to quantify the pore size of each type of scaffold. Scaffolds were prepared, frozen, and sliced using a cryostat. Each scaffold was cut into 100um slices. Slices were mounted on a glass slides simply by pressing the room temperature plate to the frozen slice. The surrounding freezing solution would melt and adhere the scaffold slice to the slide. In total, seven slices from one 125-250um scaffold, eight slices from one 250-500 scaffold, and six slices from one control slice were used in the data analysis. From each slice, three images of the scaffold pore structure were taken at specific positions on the scaffold using the Nikon SMZ 745T microscope and TSVIEW7 image acquisition software at 1x magnification. Figure 1 exhibits examples of each scaffold. The image analysis application ImageJ was used to calculate the total number of pores in one section of the slice, the average area of each pore, the total area of pores, and the percent area of pores. All original images were 1280x960 pixels. Pixels were converted to micrometers using the line tool on a 1x magnification of a ruler. Every 132 pixels equated to 1000um making each image size 9696um X 7272 um. Image analysis was performed by first converting each image to a black and white image where the black areas represented the void spaces and the white represented the scaffold. The data was gathered using the “Analyze particle” tool in ImageJ. Pore width and length were found using the line tool measuring all clearly defined pores. Most pores exhibited circular, oval, or rectangular shape. Because of the variety of pore shape, it was determined pore length would be the length of the pore at its widest point. In contrast, pore width represents the length across the pore perpendicular from the position pore length was calculated. In addition to challenges with pore shape, most pores showed interconnectivity making some pore boundaries ambiguous. The data collected from the “analyze particle” tool and the data gathered from measuring length and width of each individual pore generated the characterization of each scaffold type.

*Seeding scaffolds and cell culture*

L6 myoblast cells from rat muscle tissue were used in all cultures. Culture medium was created using Gibco Dulbecco’s Modified Eagle Medium (DMEMF12) with 10% Gibco Fetal Bovine Serum, 1% Gibco GlutaMax L-Glutamine, and 0.1% Gibco Gentamicin reagent solution. L6 cells were thawed and placed

in a T-75 flask. 10-12mL of the created DMEM/F12 was added to the culture and the culture was incubated at 37°C. Media was exchanged every 48 hours until cells reached confluency. Once cells became confluent, cells were passaged to four T-175 flasks. The confluent cells were treated with 0.25% trypsin to detach cells from the flask. Cells were removed from the T-75 flask and centrifuged at 300G's for 5 minutes. After centrifuging, 8mL of new media was used to break up the formed cell pellet. 2mL of cells were added to each T-175 flask. An additional 15mL of DMEM/F12 media was added to each flask. Cells were again allowed to reach confluency.

To seed the cells onto the scaffolds, the scaffolds had to first be sterilized. One scaffold was placed into each well of a six well plate. Each scaffold was covered in 5mL of 70% ethanol solution. The scaffolds sat in solution for 30 minutes and placed under vacuum for 15 minutes. The ethanol solution was removed and replaced with sterile Dulbecco's Phosphate Buffered Saline. Saline acted as a rinse to the ethanol, which is harmful to the cells. After three rinses, 2mL of fibronectin was added to each scaffold and incubated overnight at 4C. Fibronectin plays an important role in cell adhesion allowing cells to attach to the polymeric scaffold [12]. After sterilizing the foams, the total number of cells grown was estimated using a Bright-Line hemacytometer. The cells were diluted to a concentration of 6 million cells/mL. A total of 3 million cells per scaffold were desired. Cells were added to each scaffold drop by drop placing 0.25mL onto each side of the scaffold. After allotting time for cells to attach to the foam, 5mL of media was added to each well.

Media to promote ECM production was created by using the previously described DMEM/F12 media in conjunction with 10% ascorbic acid (AA) and 0.02% TGF beta 1 (TGFb1). Media was exchanged every 24 hours while the cells were in clear well plates. After two days the scaffolds were transferred from clear well plates to petri dishes where 2-3 scaffolds would occupy each petri dish. Once in petri dishes, media was exchanged every 48 hours. In total, six control scaffolds, five 250-500um scaffolds, and five 125-250 scaffolds were seeded and cultured.

The first cell cultures were not successful. Due to a carbon dioxide shortage in the incubator, the cultures were transferred to another incubator and were highly susceptible to contamination in transferring. Additionally, it was likely sterile culture techniques were not adequately followed leading to all cultures becoming contaminated with bacteria. A second round of cell culturing was required following the same procedure of sterilizing foams, seeding foams, and feeding foams. There were five control scaffolds, six 125-250um pore scaffolds, and six 250-500um pore scaffolds. Cells remained in culture for three weeks exchanging media every two days.

*Sacrificing cultures and harvesting ECM*

After three weeks, the sacrificial PU foam was dissolved by both physical and chemical means. Scaffolds were first frozen at -80°C. Once frozen, the scaffolds were moved to the lyopholizer and sat overnight. The following day, one control scaffold was sacrificed to determine if the resulting ECM would have adequate strength to hold together while undergoing multiple rinses to remove the PU. ECM quickly broke apart and lost its original structure. The fragility of the ECM led to submersing the remaining scaffolds in paraformaldehyde. Paraformaldahyde functioned to lock the ECM structure forming ketone bonds throughout. However, it makes the harvested ECM useless for clinical applications, as the paraformaldehyde is toxic to tissue. The scaffolds remained in paraformaldehyde for 24 hours. Scaffolds were then submersed in 5mL of DMAC. DMAC functions as a solvent to dissolve PU leaving behind the ECM structure. After 2 hours, the first rinse of DMAC was removed and replaced with a second rinse of DMAC. This set for 24 hours. Three rinses of DMAC were used replacing each rinse every 24 hours. A final water rinse was used to wash out DMAC. The resulting ECM structures were lyophilized and weighed. Images were taken of the final ECM structure using the Nikon SMZ 745T microscope at 1x magnification.

*Statistics*

Testing groups were compared using two-tailed student's T-test. Acceptance criteria for statistical significance required p values less than 0.05. Pore length, pore width, area covered by void spaces, and ECM yield were measured. All graphs represent mean values with standard error bars.

**Results**

The characterization of the scaffolds was the first priority to demonstrate that the sugar sieveing and templating approach provided a means to create sacrificial scaffolds with targeted pore sizes. Porosity was measured by calculating the density of each scaffold as described previously and applying the values to equation 1. The results were not statistically significant (data not shown).

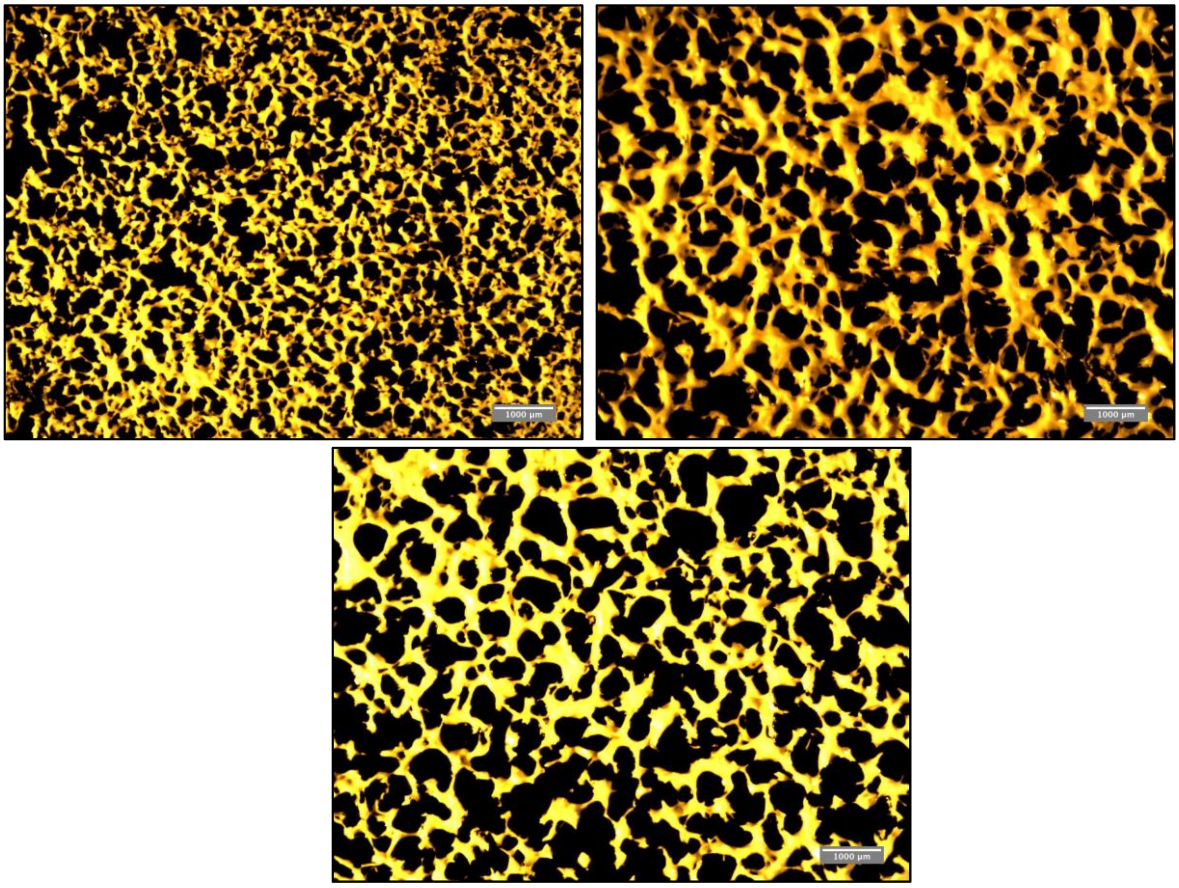


**Figure 1.** Characterizing Polyurethane scaffolds using ImageJ. Image of one 100um slice of PU scaffold at 1x magnification for 125-250um scaffold (top left), 250-500um scaffold (top right), and Control scaffold (bottom)

The area of void space (%) from the ImageJ analysis was compared and shown in Figure 2. For a two-dimensional slice, the control scaffolds (n=17) had the highest percent coverage at 67.3% ± 1.1% showing it had the highest porosity. The 250-500um (n=18) scaffolds had an average percent area covered of 62.9% ± 1.2% and the 125-250um (n=17) pore scaffolds had an average percent area covered

of 59.4% ± 0.8%. The highest p value calculated between scaffolds was 0.0013 showing each group was statistically significant.

The average length and width of an individual pore in each scaffold showed far larger differences. The control (n=357) had pores of average length and width of 551.3 ± 6.3um and 387.8um ± 4.5um respectively. 250-500um (n=434) scaffolds had an average pore length and average pore width of 435.2±4.4um and 310.6± 3.0um. 125-250um (n=577) scaffolds had an average pore length and width of 270.7 ± 2.7um and 191.3± 2.0um respectively. The 250um-500um exhibited a 20% decrease in width and 21% decrease in length. 125-250um scaffolds exhibited a 50% decrease in both individual pore width and length compared to the control. All p values were less than 0.00001 showing statistical significance across each group.

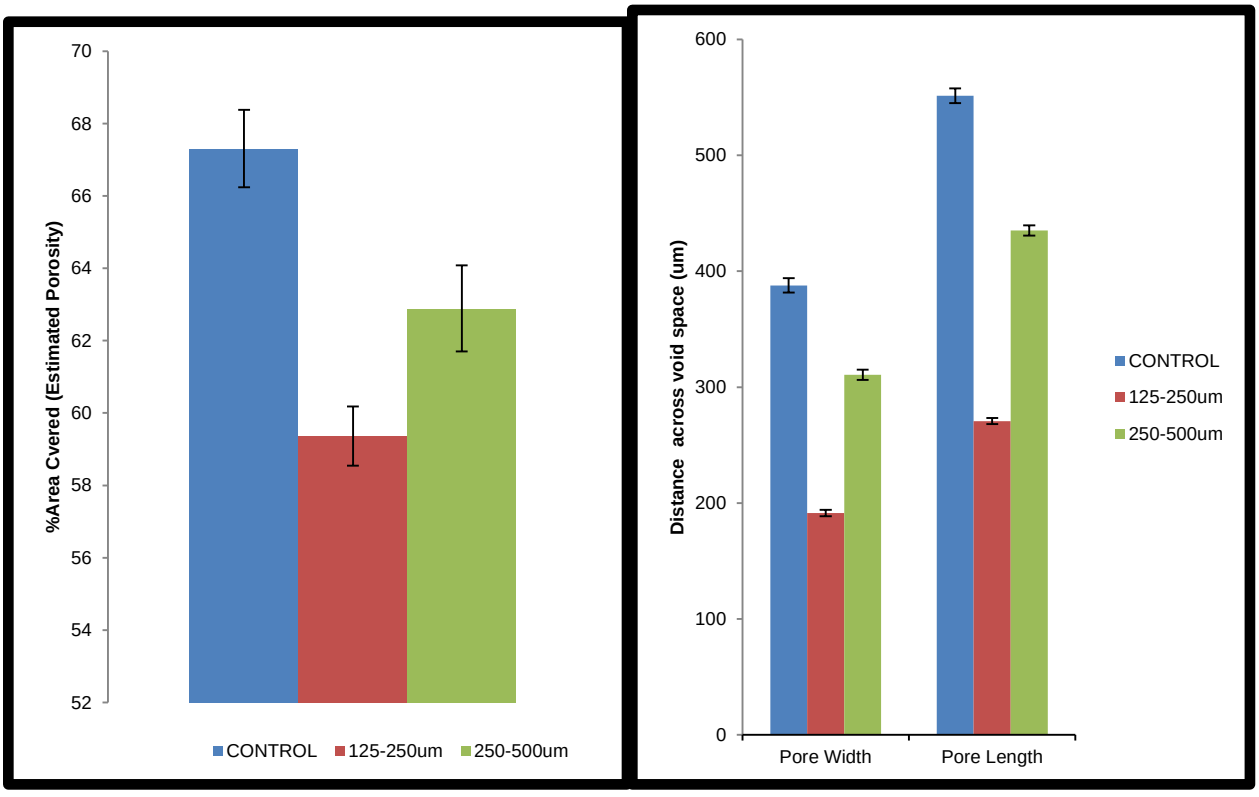


**Figure 2.** ImageJ analysis of pore structure. On left, the average area covered by void spaces (% porosity) shows the control had the greatest area of void spaces. 125-250um scaffolds had the least amount of void spaces. On right, the average pore length and width are shown (um). Again the control had the largest average pore size and 125-250um scaffolds had the smallest average pore size.

The ImageJ data, specifically for individual pore size, confirms each scaffold type is structurally different from each other. A histogram was collected for both pore length and pore width. Pore size for each scaffold was also similar to the size of sugar granules used to make the scaffold. Figure 3 shows that most pores in the 125-250um scaffolds contained pores between 100-300um. 69.7% of all pore widths and 51.8% of all pore lengths were contained inside the 125-250um bounds. Overall, 89.6% of pore widths and 68.8% of pore lengths were between 100-300um. 250-500um scaffolds had a broader range of pore sizes, but most fell between 200-600um. 73.7% of pore widths and 55.1% of all pore lengths fit inside the defined 250-500um bounds. 89.9% of pore widths and 75.6% of pore lengths in these scaffolds fell between 200-600um. The control group had the broadest range, as pore size appears to be random throughout all ranges specifically when looking at pore length. For control scaffolds pore length, only one category contained more than 10% of all pore lengths (550-600um at 12.0%). Looking at a 250um span, the largest percentage of pore lengths in the control scaffolds occurred from 350-600um with an overall of 42.9% of all pores being found in this range. For pore width in control scaffolds, this range occurred at 300-550um and contained 57.4%. In comparison, the largest percentages for the same criteria for 125-250um scaffolds and 250-500um scaffolds were as follows: Pore width 100-350um contained 89.6% of all pores, pore length 150-400um contained 79.2% of all pores, pore width 200-450um contained 69.1% of all pores, and pore length between 250-500um contained 55.1% of all pores.

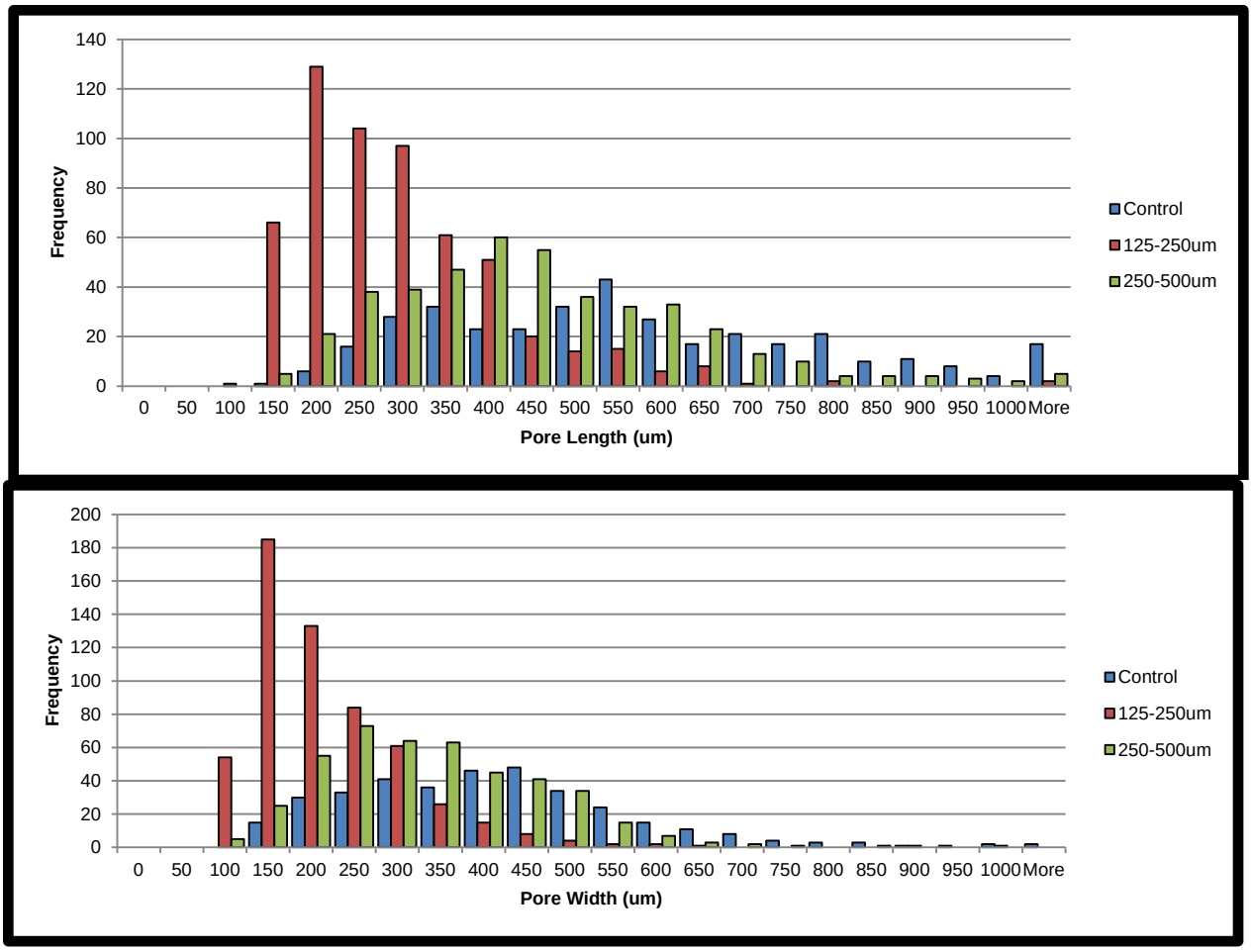


**Figure 3.** Histogram of pore length (top) and pore width (bottom for all pores analyzed in ImageJ. Clear peak values for 125-250um scaffolds occur between 100-300um and for 250-500um scaffolds between 200-600um.

Material yield differences between each scaffold were statistically insignificant. Extracellular matrix production was highest with the control scaffolds (n=4) at 4.15mg ±0.44 mg. 250-500um pore scaffolds (n=6) and 125-250um pore scaffolds (n=6) averaged 3.82mg±0.50mg 3.55mg±0.27mg extracellular matrix accumulation, respectively. Although quantitative data for ECM structure from each scaffold was not gathered, visually ECM all had similar structures from each scaffold. In comparing each group, the calculated p value between 125-250um scaffolds and 250-500um scaffolds was p=0.47. The p value between 250-500um scaffolds and the control was p=0.48. The p value between 125-250um scaffolds and the control was p=0.14. Definitive relationships cannot be gathered; however an overall trend is shown for increased ECM yield with increasing pore size.

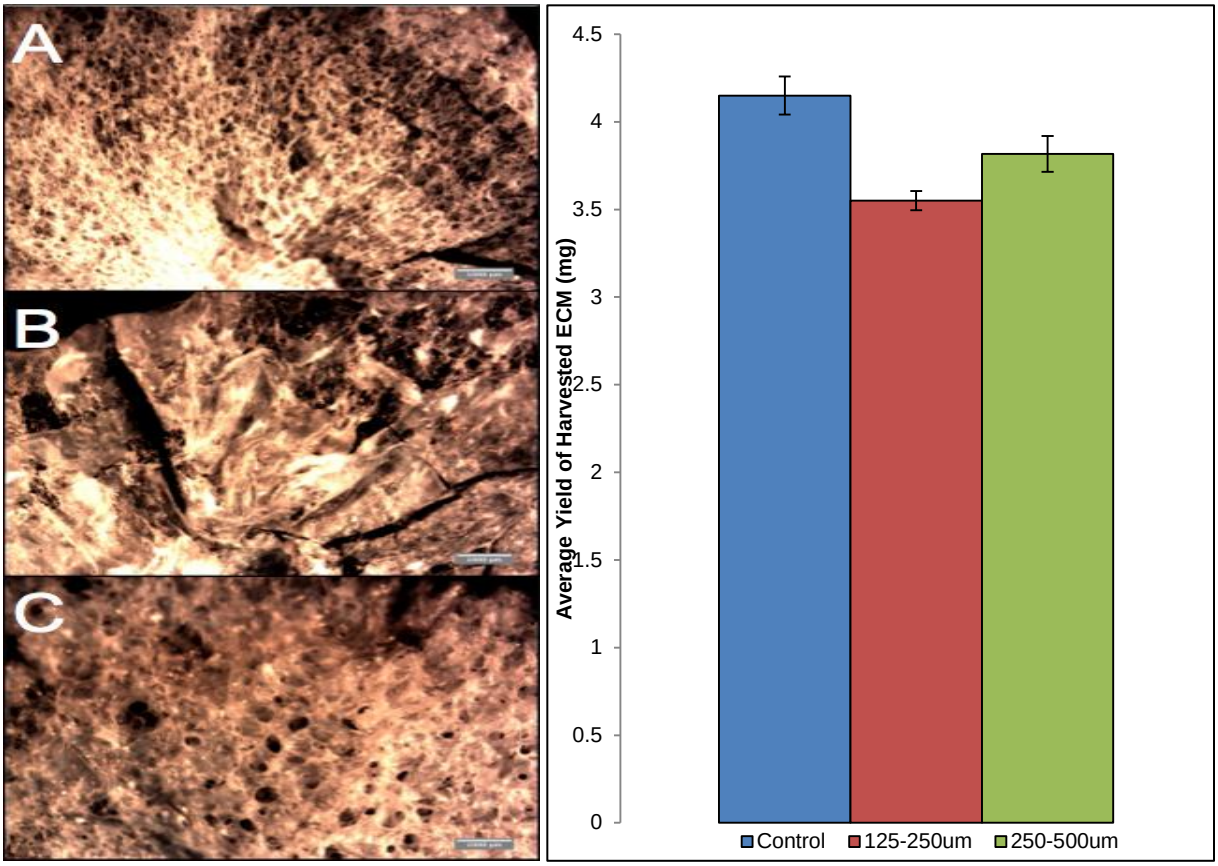


Figure 4. ECM yield from each PU scaffold type. On left, 1x magnification images gatherd of ECM gathered from sacrificed A)125-250um scaffolds B)250-500um scaffolds and C) Control scaffolds. On right, average ECM yield for each scaffold group.

**Discussion**

Natural polymer scaffolds as a biomaterial in tissue regeneration provides an environment cells can recognize, remodel, and proliferate through. Natural scaffolds are advantageous over synthetic polymers because synthetic polymer scaffolds are known to cause a foreign body response. The response can cause fibrous encapsulation and chronic inflammation. In this study, we sought to improve ECM production from cell cultures growing in sacrificial PU scaffolds by controlling PU scaffold pore size. The ECM produced from the cultures can then be used as a viable alternative to synthetic polymer scaffolds for tissue regeneration. Maximizing ECM production will improve the feasibility of using this method at a larger scale for tissue regeneration scaffolds. It was hypothesized that adjusting the pore size of PU scaffolds would affect ECM yield, however it was not known whether smaller or larger pore size would increase or decrease. The results found in this study suggest that larger pore size leads to higher ECM production. This is similar to results previously reported by Lien et al. where larger pores were shown to

cause cells to have higher production of ECM while smaller pores caused cells to proliferate at a higher rate [13].

To show if pore size had an effect on ECM production, we first sought to prove the efficacy of a particle leaching method in creating a PU scaffold for cells to grow and produce ECM. Previous studies have reported a multitude of methods for creating porous scaffolding. These methods include solvent casting followed by particle leaching, lyophilization, gas foaming, and electrospinning [14]. This study focused on solvent casting with particle leaching. The basic method described previously involves compacting soluble particles, pouring a polymer solution over the particles and rinsing out the particles with a solvent leaving behind void spaces. Salt is the most common particle used, however in this study sugar was used citing the low density of sugar keeps particles from sinking in polymer solution and concentrating at the bottom of the scaffold [15]. Moreover, the composition of the particle has been shown to affect the interconnectivity of the pores and more responsive to cell proliferation [16,17]. Sieving sugar granules proved to be an effective way to leave void spaces behind of a desired pore size in the PU scaffold. This matched previous reports. Outliers did occur likely stemming from pore connectivity, pores collapsing when cut by the cryostat, or from sugar granules that did not fall through the sieve when separating sugar granules. The data gathered clearly showed the highest peaks of pore sizes within the respected range of sugar granule size used. These findings support the use of the sugar templating approach for the fabrication of sacrifical polymer foams with targeted pore sizes.

Our results for ECM yield were not deemed statistically significant across each PU scaffold size. In spite of this, an overall trend of increased ECM yield was observed in larger pore size. This is compatible to previous studies performed where scaffolds with larger pore size reported higher yields of ECM byproducts [13,15,18]. Large pores in scaffolds are known to allow easier diffusion of nutrients to cells in the scaffold. Nevertheless, these cells can have limited sites for cell attachment compared to smaller pore sizes [13]. The lower ECM totals for smaller pore size suggest cells were sterically hindered in producing more ECM. On its own, eukaryotic cells are approximately 100um in diameter. A pore size around 125um leaves cells little room to produce ECM. The cells are also held tightly to the PU scaffolds coated with

fibronectin. The PU scaffold makes it likely cells need a minimal amount of additional structure to support cell proliferation. Lien et al. reported higher cell densities in gelatin scaffolds at similar small pore sizes (50-150um, 100-200um), but saw cells in larger pore scaffolds secreted 2-5 fold more ECM than cells in smaller pore sizes [13]. It has been reported that smaller pore sizes tend to cause cell proliferation. Specifically, Oh et al. reported fibroblasts cells prefer growing at smaller pore sizes [17]. Meanwhile, larger pore sizes lead to cells producing ECM [13]. Many of the larger pores showed extensive interconnectivity, which is likely to promote better diffusion of nutrients [18]. The diffusion of nutrients and increased metabolism allows these cells to maintain a normal physiology and have increased ECM growth [13].

Overall, the outcomes of this study show a defined method in creating PU scaffolds for cell culture with targeted pore size and the relationship of this pore size to overall ECM production. Factors that could have influenced the results outside of pore size could be the interconnectivity of the pores in the PU scaffolding. The improved diffusion of nutrients to cells could allow cells to proliferate faster, requiring increased ECM to sustain all cells. However, studying the interconnectivity of the pore structure was outside the scope of this study and should be investigated in the future. Further, the data acquired came from relatively small sample sizes. A statistically significant result could be found if the procedure was repeated with a larger sample size. A future direction for this research will be to examine larger and larger pore sizes (500-750um, 750-1000um) to optimize an upper bound in PU scaffold pore size. Moreover, the ECM produced must have its performance study in vivo in animal trials. L6 rat fibroblast cells were used in this study. The ECM gathered from PU scaffolds of varying pore size need to be implanted into injured rat musculoskeletal tissue to compare cell proliferation, and tissue histology in vivo. ECM harvested from scaffolds with smaller pore size may enhance overall tissue regeneration despite producing less ECM making it more advantageous.

**Acknowledgements**

This study was performed under the guidance of Dr. Jeffrey C. Wolchok. All materials were provided through his lab at the University of Arkansas at Fayetteville, Arkansas.

[1] Hubbell JA. Biomaterials in Tissue Engineering. Nature. 1995; 13(6): 565-76.

[2] Badylak SF. The extracellular matrix as a scaffold for tissue reconstruction. Semin Cell Dev Biol. 2002; 13(5): 377-83.

[3] Badylak SF. Regeneerative medicine and developmental biology: the role of the extracellular matrix. Anat Rec B New Anat. 2005; 287(1): 36-41.

[4] Xiaohua L, Holzwarth JM, Ma PX. Functionalized Synthetic Biodegradable Polymer Scaffolds for Tissue Engineering. Macromlecular Bioscience. 2012; 12(7): 911-19.

[5] Balachandran, K. 2/12/14 Wound Healing. Advanced Biomaterials and Biocompatibility. University of Arkansas, Fayetteville, AR. 02/12/2014. Lecture.

[6] Wolchok JC, Tresco PA. The isolation of cell derived extracellular matrix constructs using sacrificial open-cell foams. Biomaterials. 2010; 31(36): 9595-603.

[7] Badylak SF, Freytes DO, Gilbert TW. Extracellular matrix as a biological scaffold material: Structure and function. Acta Biomaterilia. 2009; 5(1): 1-13.

[8] Hodde J. Naturally Occurring Scaffolds for Soft Tissue Repair and Regeneration. Tissue Engineering. 2002; 8(2): 295-308.

[9] Wolchok JC, Tresco PA. Using growth factor conditioning to modify the properties of human cell derived extracellular matrix. Biotechnology Progress. 2012; 28(6): 1581-87.

[10] Karageorgiou V, Kaplan D. Porosity of 3D biomaterial scaffolds and osteogenesis. Biomaterals. 2005; 26(27): 5474-91.

[11] Lubrizol. MSDS Tecoflex SG-80A. 2013. https://www.lubrizol.com/LifeScience/Products/Tecoflex.html#

[12] Dolatshahi-Pirouz A, Jenson T, Kraft DC et al. Fibronectin Adsorption, cell adhesion, and proliferation on nanostructured tantalum surfaces. ACS Nano. 2010; 4(5): 2874-82.

[13] Lien SM, Ko LY, Huang TJ. Effect of pore size on ECM secretion and cell growth in gelatin scaffold for articular cartilage tissue engineering. Acta Biomaterialia. 2009; 5(2): 670-79.

[14] Annabi N, Nichol JW, Zhong X, et al. Controlling the Porosity and Microarchitecture of Hydrogels for Tissue Engineering. Tissue Eng Part B Rev. 2010; 16(4): 371-83.

[15] Horak D, Kroupova J, Miroslav S et al. Poly(2-hydroxyethyl methacrylate)-based slabs as a mouse embryonic stem cell support. Biomaterials. 2004; 25(22): 5249-60.

[16] Suh SW, Shin JY, Kim J, et al. Effect of different particles on cell proliferation in polymer scaffolds using a solvent-casting and particulate leaching technique. ASAIO Journals. 2002; 48(5): 460-64.

[17] Oh SH, Park IK, Kim JM, Lee JH. In vitro and in vivo characteristics of PCL scaffolds with pore size gradient fabricated by a centrifugation method. Biomaterials. 2007; 28(9): 1664-71.

[18] Griffon DJ, Sedighi MR, Schaeffer DV, et al. Chitosin scaffolds: interconnective pore size and cartilage engineering. Acta Biomaterialia. 2006; 2(3): 313-20.